Fault Structure and Fluid Flow (Stops 5, 7 and 9)

Russell Davies and Brann Johnson

October 2026

Introduction

This section of the field guide discusses the regional structural geometry as relates to the Green River Anticline trapping configuration and fault zone architecture and relationship of the two in controlling the fluid migration in reference to Field Stops 5, 7 and 9.

Structural Traps: General Introduction

A requirement for a successful oil and gas discovery or CO_2 sequestration project is a trap. The trap includes a structural closure, a top seal or caprock and, if faulted, a lateral seal. The simplest trap is an anticline with dipping closure in all directions.

Consider the topographical map of an anticline on a subsurface horizon top in Figure 1. Hydrocarbons or CO_2 generated from a deeper source or injected into this anticlinal trap will fill a maximum area from the crest of the structure to the lowest closing contour. If these fluids fill to the base of the structure it is filled to spill and will leak out at the northwest or southeast open contour.

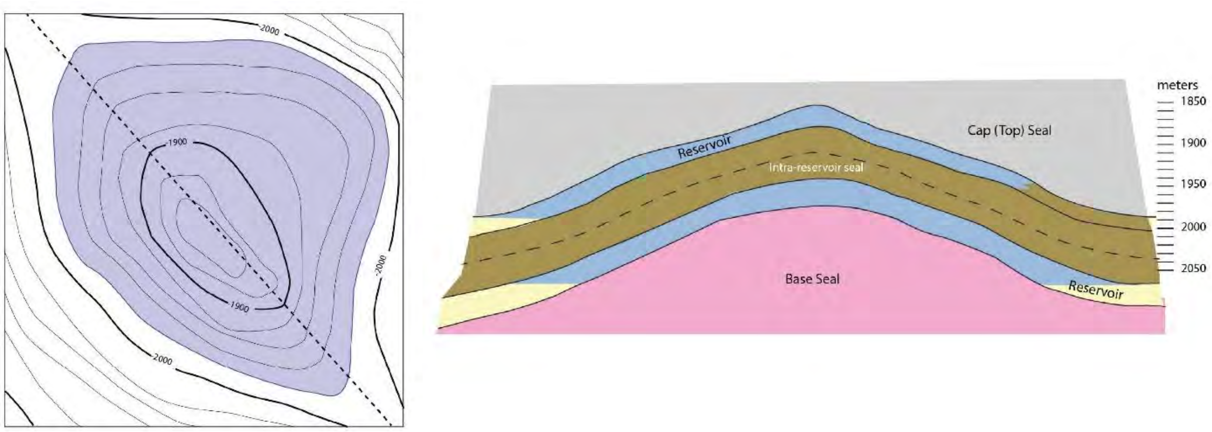

Figure 1. An example of a simple unfaulted anticlinal trap with a broad cap rock or top seal and intrareservoir seals restricting the upward migration of the CO_2 or hydrocarbons. The limits on the column heights is the spill point to the NW or SE.

A caveat of this fill-to-spill model is a required caprock or low permeability lithofacies such as a mudrock across the crest of the structure to act as a top seal to restrict vertical fluid loss. In the case of hydrocarbons or CO_2, the fluids are lighter than the brine in the pore spaces and rises by a buoyancy force displacing the brine and migration vertically through a more permeable caprock but sealed by a low permeability lithofacies such as a mudrock.

In this example (Figure 1), CO_2 is constrained within two porous reservoir sandstones as shown in yellow with the CO_2 fluid in blue. The two reservoirs are separated by an intra-reservoir seal (brown) with a caprock (grey) as a top seal. With sufficient height of CO_2 or hydrocarbons in the trap, the buoyancy pressure between the base of the fluid column and the crest of the structure may exceed the capillary entry pressure of the caprock, resulting in displacement of brine from the caprock and leakage of fluids through the seal. Because CO_2 and hydrocarbons are immiscible with brine, capillary forces control the initial displacement of brine by the nonwetting CO_2 or hydrocarbon phase through the caprock pore system. Once the nonwetting phase enters the caprock, the rate and distribution of flow are controlled in part by relative permeability, which varies as a function of CO_2 or hydrocarbon saturation relative to brine.

A riskier trap, or one more likely to leak is a faulted anticline (Figure 2). In this example, the anticlinal trap is cut by multiple faults. Those near the crest of the structure have low displacement where reservoirs are juxtaposed across the faults with a potential for cross-fault communication or leakage. If these faults cut across an anticline with a structural closure in all directions (four way closure) the trap may not be compromised. However, a risk is fluid loss up the faults and out of the trap.

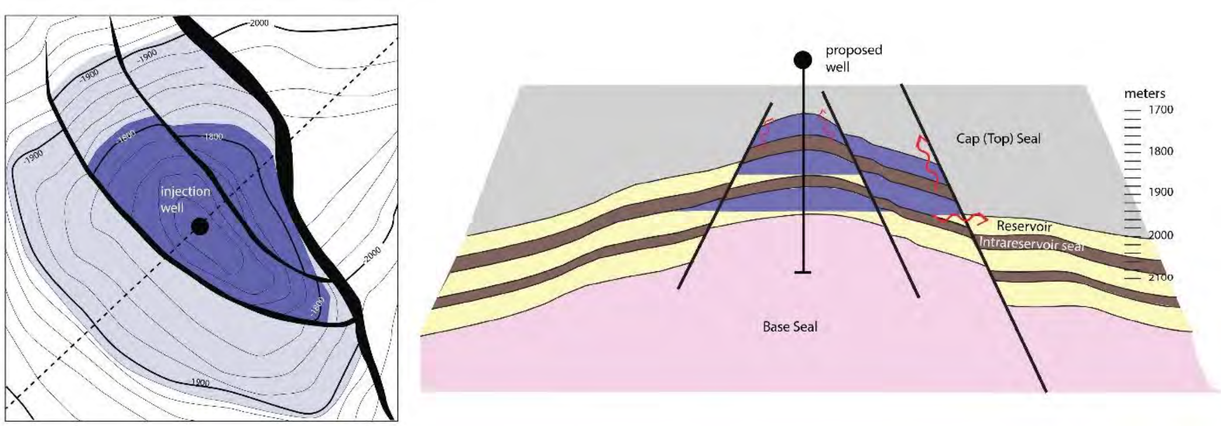

Figure 2. An example of a faulted anticline. Small faults at the crest of the anticline are potential migration pathways for the leak of the buoyant CO_2 or hydrocarbons. The larger throw fault must seal below the contour closure in dark blue or the fluids will be lost across the fault.

A larger throw fault, to the right on the contour map juxtaposes the upper section of the upthrown reservoirs in the footwall of the fault against a caprock on the downthrown side or the hanging wall. This is considered a juxtaposition seal limiting or restricting cross-fault flow. The lower upthrown reservoirs are juxtaposed against reservoir on the downthrown side of the fault where cross-fault flow is a risk. In this scenario the hydrocarbons or CO_2 as represented as blue in the figure may be sealed against the large throw fault from cross-fault leakage because of the juxtaposition of the caprock against the reservoirs. However, if the fluids leak across the fault where the reservoirs are juxtaposed deeper in the section there is no trap on the downthrown side and the trap is compromised. A low permeability gouge or clay smear between the juxtaposed reservoirs may act to seal the fluids on the upthrown side of the fault. An up-fault flow low of fluids is a risk for all the faults.

Green River Anticline Trap

This scenario of a faulted anticline is like the structural style in the field trip location. As is shown clearly on the geological map (Figure 3 and Plate 1), an anticline (referred to as the Green River anticline by Kampan et al., 2014, Shu 2018, and others) is cut by several faults. The plunging nose of the anticline creates a structural closure to the north. The northernmost plunging nose of the anticline is offset by the Little Grand Wash Fault that dips to the south. The fault is curved with a concave shape to the north but oriented approximately east west with a 60 km length (Urquhart, 2011), normal offset and maximum stratigraphic throw of approximately 200 meters (Vrolijk et al., 2005). In outcrop, the Cretaceous Mancos section in the hanging wall is juxtaposed against the Jurassic Morrison Formation in the upthrown footwall to the north along the central part of the fault with the largest displacement. The throw along a fault varies and, therefore, the stratigraphic juxtapositions change along the fault length.

The shape of the plunging anticline displaced across the Little Big Wash Fault is repeated to the south in the hanging wall. This downward displaced plunging nose of the anticline is cut by a set of faults to the south that are nearly straight in map view oriented WNW-ESE. The northernmost faults bounding the Salt Wash Graben (Figure 3) are a focus of this field trip.

The structural styles of the faulted anticline is like the faulted trap described in Figure 2.

Ten Mile and Salt Wash Graben

The set of faults cutting across the southern nose of the plunging anticline form narrow grabens approximately 1 km wide. Faults bounding the graben to the north are closely spaced with small overlaps at their tips and dip to the south with normal offset. A second set of faults to the south dip to the north forming the southern boundary of the graben.

The graben along the strike is sometimes separated into two (Williams, 2004; Jung et al., 2015), the Salt Wash Graben to the west and Ten Mile Graben to east, although they are likely kinematically related. The San Rafael Desert and Moab 30' X 60' quadrangle maps by Doelling et al., (2015) and Doelling (2002) refers to only a single Ten Mile Graben and Shipton et al., (2004) labels the grabens as Salt Wash Faults. We adopt the Williams (2014) labelling with two grabens (Figure 3 and Plate 1).

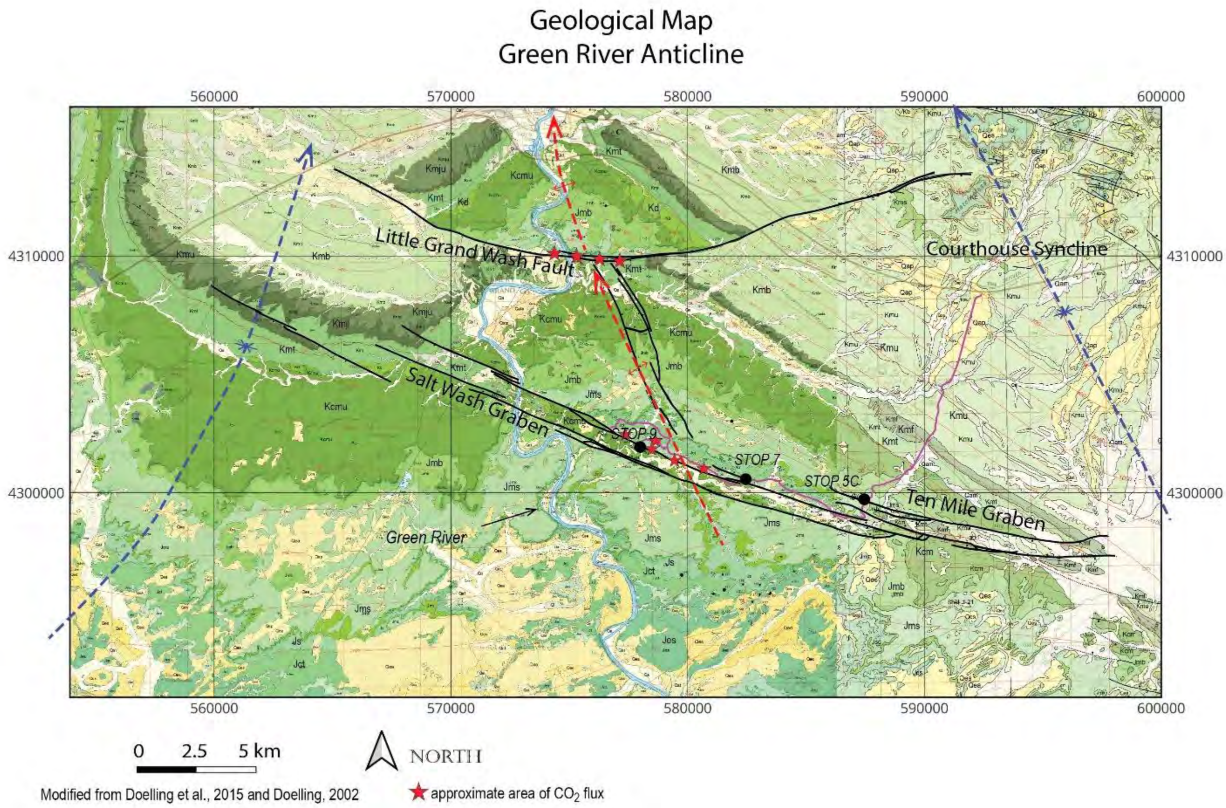

Figure 3. Geological map of the faulted Green River anticline with the principal faults hightlighted and the main structures labelled. Modified from Doelling et al, 2015 and Doelling (2002).

The faults bounding the Salt Wash Graben to the west are not single traces across the mapped surface but instead comprised of separate segments with a combined length of approximately 22 km. The segments interact at their tips with small overlap or distance between the fault tips, and separation or the distance separating the fault traces. These overlaps are called relays and form relay ramps where the displacement on one fault is shared across the ramp with the second (Davies et al., 1997). If the fault tips connect across the relay this is called a hard link and if they are not physically connected a soft-link (Figure 4). Both types of relays are observed along the faults bounding the grabens. The Salt Wash Graben extends west of the Green River. At the western boundary its southern bounding fault is offset at its tip to the south to a normal fault dipping south that extends westward for approximately 9 km.

Approximately 30 km east at the mapped termination of the Salt Wash Graben the Ten Mile Graben extends along the same trend but offset to the north (Figure 3 and Plate 1). The south dipping normal fault bounding the Salt Wash Graben to the north shares displacement across a relay to the north dipping normal fault bounding the Ten Mile graben to the south. The Ten Mile graben has a strike length of approximately 8 km.

The south dipping, northern bounding fault of the Salt Wash Graben has the larger stratigraphic throw. Along most of the trace of this fault in the field trip area, the fault juxtaposes Upper Entrada in footwall against Cedar Mountain in the hanging wall. This corresponds to a stratigraphic throw of about 350 meters. The stratigraphic throw on the north dipping, southern bounding fault is approximately 140 to 190 meters, which places either the Salt Wash member or Tidwell member of the Morrison in the footwall and Cedar Mountain in the hanging wall along most of the fault trace. The larger estimated throw is in the eastern portion of this bounding fault.

A graben bounded by normal faults with low throws extends between the Little Grand Wash faults and the Salt Wash Graben and extends along the plunging nose of the anticline with an orientation of NNW-SSE. The bounding faults to this graben are also comprised of multiple closely-spaced segments. This graben may have formed in response to the bending of the section along the axial crest of the anticline.

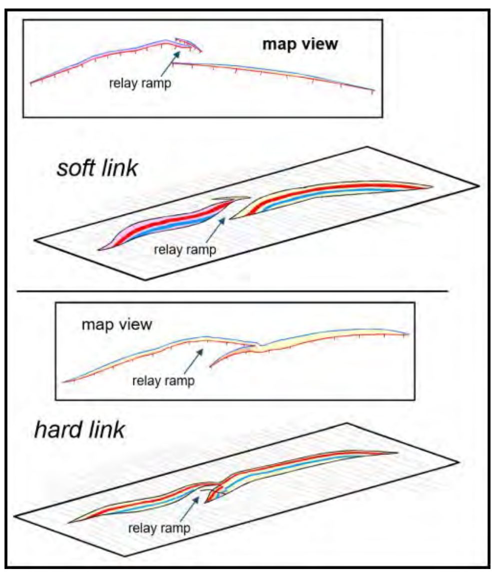

Figure 4. Conceptual models of map view and perspective views of fault tip connection across relays as soft link or unconnected fault tips and hard link or physically connected tips.

Green River Anticline: Structural Trap

A contour map across the Green River anticline derived from the structural contours on the Doelling et al., (2015) and Doelling (2002) geological maps on the top Navajo Sandstone (Figure 5 and Plate 2) clearly shows the structural geometry in the subsurface. The structure forms a trap like that described in the text above and in Figure 3. Lighter fluids such as CO_2 can fill a permeable and porous reservoir from the structural crest to the base of the structure defined by the lowest closing contour if the Little Grand Wash fault is sealing along its length. This area from the structural crest to the lowest closing contour is shown by the light blue polygon labelled A in Plate 2 and Figure 5. Sealing along the fault may occur from the juxtaposition of upthrown reservoirs against downthrown sealing lithofacies (Figure 3) or if the fault develops a low permeability fault-rock from the mixing or smearing of high clay content rocks cut by the fault. The buoyant fluids may also leak through an overlying caprock or up the fault resulting in losses to shallower reservoirs or the surface.

Fluids leaking across the Little Grand Wash Fault would migrate into reservoirs on the southern nose of the Green River Anticline with a similar north dipping closure and southern closure defined by the faults bounding the Salt Wash and Ten Mile grabens. These faults would have to seal or else the fluids would leak across the faults to the south where the structure shows no trapping closure. The blue polygon (Plate 2; Figure 5) across this southern nose of the anticline labelled C in the figure defines the limit from the structural crest to the lowest contour to the east assuming the faults seal. If the reservoirs are in communication across the Little Grand Wash Fault the fluids would have the same limiting contour to the north, which is shown as the darker blue polygon in the northern dipping nose of the anticline (labelled B). The polygon D in the figure represents a fill in the graben.

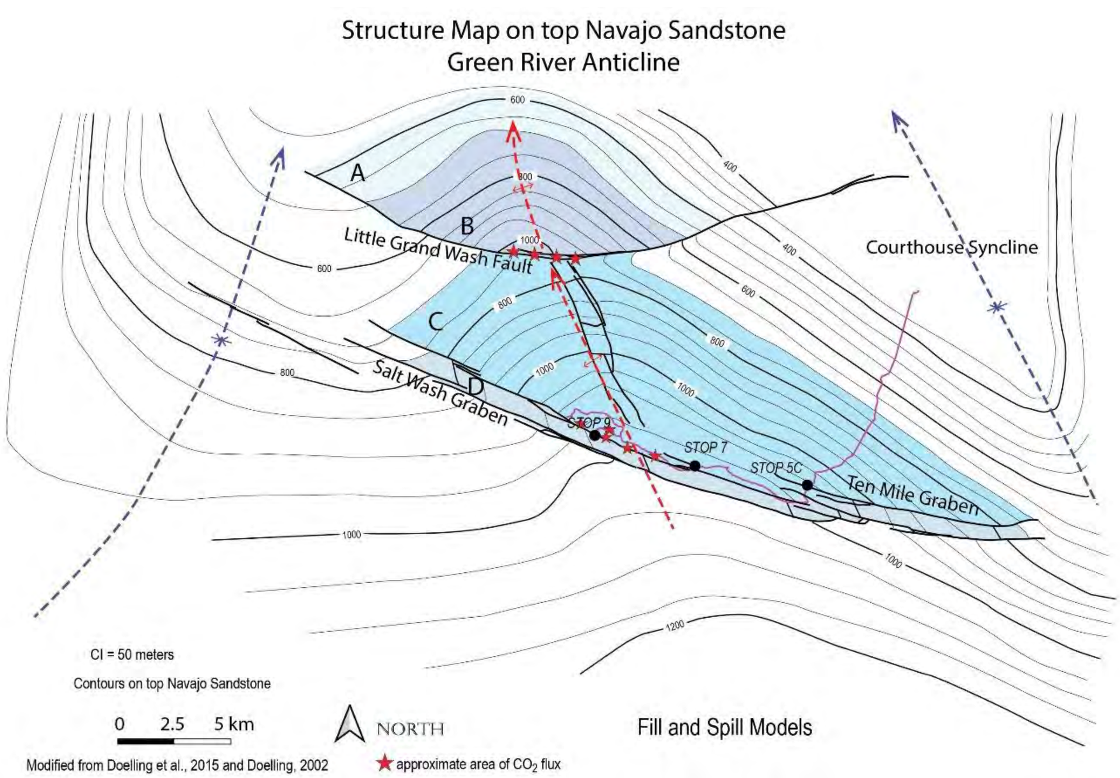

Figure 5. Structural contour map across the Green River anticline with contours on the top Navajo sandstone. The filled polygons show the maximum spill limits labelled A,B,C and D. The contours are modifed from Doelling et al., 2015 and Doelling (2002).

This discussion considers the trapping geometry from the structural styles without fluid and migration pathways. In the next section, we discuss the details of the trap styles, caprocks and fault zone architecture for mechanisms of cross-fault and up-fault flow.

Fluid Migration

Studies of fluids that have migrated to the surface in this area show that CO_2 is generated deeper in the section in the more carbonate-rich Pennsylvanian Honaker Trail, Paradox and possibly Mississippian age formations and migrate upwards with saline brines to porous reservoirs in the Jurassic Navajo and Entrada sandstones (Kampan et al., 2014 and others – see field guide reference list for complete list of studies). The CO_2 exsolves at these shallower depths and escapes to the surface. A key question is what are the migration pathways?

The geochemistry of the CO_2 generation from the deeper section is discussed elsewhere in the field guide but like an oil and gas source rock, the CO_2 is released from a host rock and migrates vertically and up dip through large pore throats or fractures in the rock volume displacing the brine by capillary processes. The migration pathway is that of least resistance or largest connected pore throat or connected fractures.

The CO_2 will migrate through porous, permeable reservoirs until it reaches a lithofacies with low permeability or small pore throats such as a mudrock. This is a caprock or top seal that limits or stops the upward migration. If the caprock conforms to a trap closure such as an anticline (Figure 1), the CO_2 will fill the reservoir capped by the top seal until its buoyancy pressure overcomes the resistance of the small pore throats in the caprock or spills from the lowest closing contour in the trap (Figure 1). If the buoyancy pressure of the CO_2 or hydrocarbons exceeds the capillary threshold pressure of the seal, the fluids will migrate across the seal at a rate dependent on the relative permeability of the nonwetting phase as a function of fluid saturation. Previous studies have suggested that the Carmel or Brushy Basin Formation overlying the Navajo sandstone and the Summerville Formation overlying the Entrada sandstone are intra-reservoirs seals limiting the upward migration and trapping the CO_2 in the respective underlying reservoirs (Jung et al., 2015).

In the case of the Green River Anticline, the reservoir is faulted with the structural crest offset against a fault (Plate 2; Figure 5). To restrict cross-fault flow and preserve the CO_2 in the trap, the fault must seal. However, there is evidence from outcrop studies along the Little Grand Wash Fault that fluids also migrate up the fault zone (Urquhart, 2011). If the fault and associated deformation such as connected fractures have a higher permeability or lower flow resistance to the caprock, the fluids will select this path of least resistance to shallower reservoirs and then to the surface.

Before discussion of potential migration scenarios, however, it is worth discussing fault zone architecture and potential mechanisms for cross-fault and up-fault flow and seal.

Fault Zone Architecture

Our impression of a fault is often biased from introductory geology where they are described as planar surfaces that offset a stratigraphic interval. In detail, however, most faults have a much more complex architecture and are typically described as a zone with a damage zone separating a fault-core of comminuted fault-rock from the undeformed protolith and often one or several discrete slip surfaces (Figure 6A; Caine et al., 1996). Although this fault model is often used to describe faults in all settings it is best applied for faults cutting a more homogeneous low porosity rock such as a granite or platform carbonate.

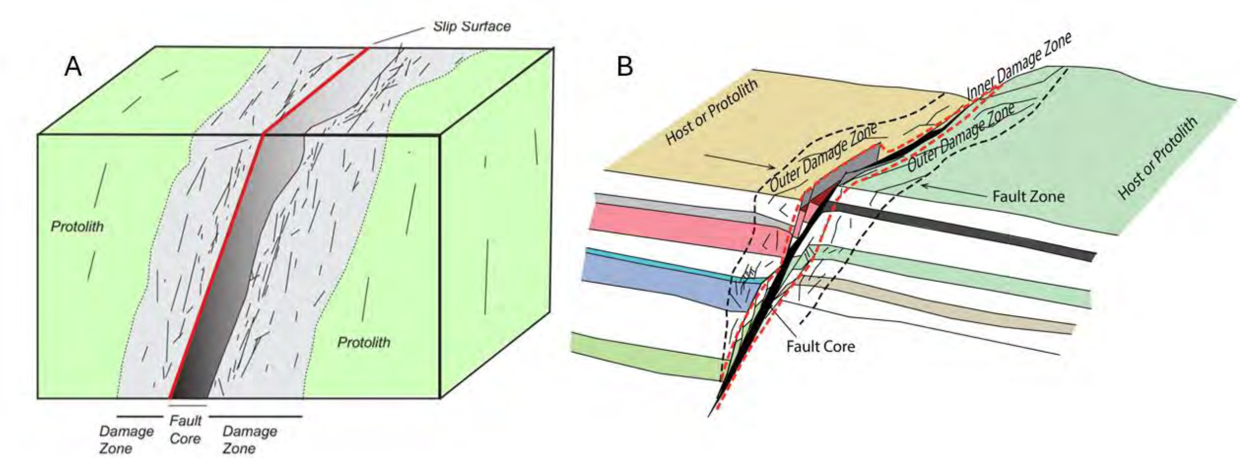

Figure 6. Fault models. A. A standard fault model most frequently described in the literature but relevant to more homogeneous, unlayered brittle sections or layered stratigraphy with limited mechanical differences between the layers. B. A complex fault model of the deformation styles expected for a fault zone crossing a layered section with greater mechanical strengths between the layers from brittle to ductile.

Where a fault cuts a more heterolithic section such as layered sandstones and shales, the fault zones are often more complex (Figure 6B). The greater the mechanical or strength differences between the layers or higher the vertical mechanical heterogeneity (VMH), the higher the complexity. These faults zones are described by an outer damage zone at the edge of the undeformed protolith, an inner damage zone, a fault-core and slip surfaces.

The outer damage zone is a width of deformation away from the central core of the fault extending up to a maximum distance of 50 to 100 meters. The damage zone is typically defined by sets of small Mode I or open fractures or small faults with a density that typically decreases with increasing distance from the fault-core. The strike of the small fractures or faults in the damage zone is most often subparallel to the strike of the main fault.

The inner damage zone, if present, is deformation of the protolith or offset stratigraphy that is rotated and attenuated into the fault-core. More ductile layers such as mudrocks are continuously sheared and brittle sandstones are offset by small faults that offset the sandstone as discrete blocks shearing both into the fault-core. The fault-core is the central narrow zone of the fault with sheared and broken mixed stratigraphy called fault-rocks. Discrete slip surfaces are often observed within the fault-core with large displacement.

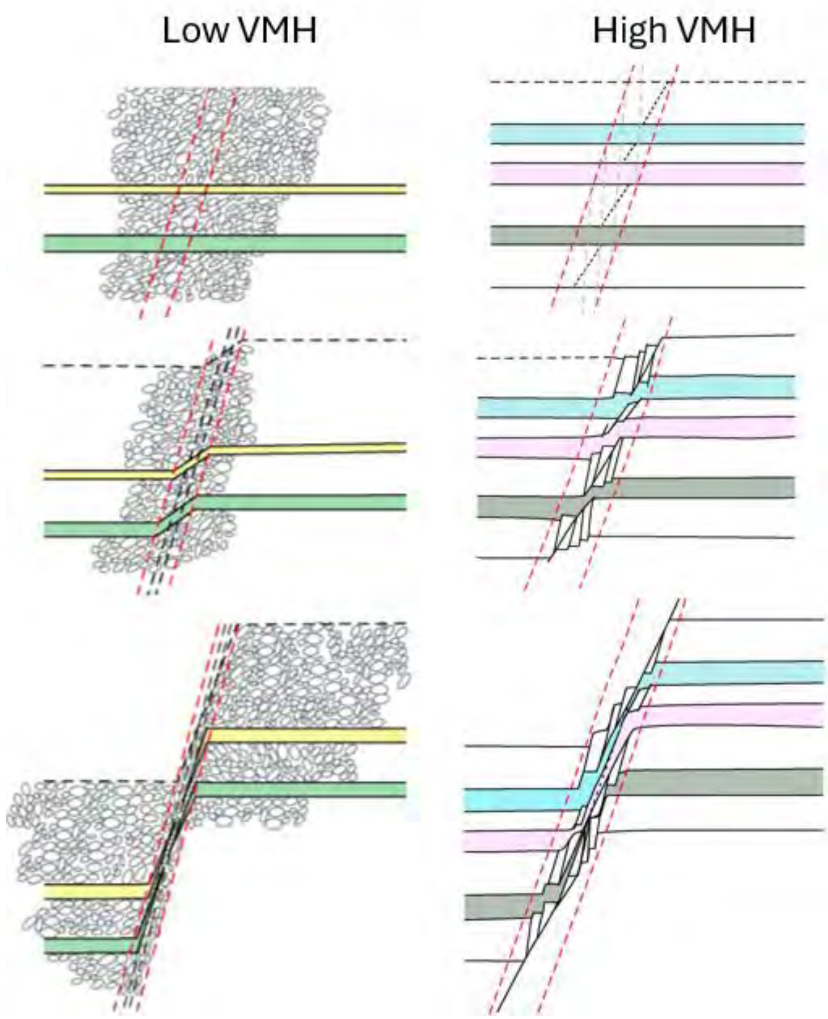

Figure 7. Evolution of fault models with differences in the vertical mechanical heterogeneity (VMH).

Fault Zone Model

Models for the evolution of faults in a layered stratigraphic section depends on the differences in the mechanical properties of the stacked layers at the time of deformation (Figure 7). For instance, at shallower depths of burial during early deposition the properties of sandstones and shales are more similar because they have not been buried deeply enough for significant compaction and cementation. Thick aeolian or turbidite sandstones, platform carbonates and granites are not layered but are also more homogeneous with similar properties. Faults cutting these sections tend to shear the layers through a zone with subsequent slip surfaces with the largest displacement. This model is shown for low vertical mechanical heterogeneity (VMH) as in Figure 7 and is consistent with a standard fault zone model as shown in Figure 6A.

With increased depth of burial, the sandstones and shales compact, but the shales maintain ductility and the sandstones become more brittle as the contacts at grain boundaries form cement sutures strengthening the rock. Faults cutting these alternating weak and strong layers at greater depths form a narrow shear zone of offset (Figure 7). The initial offset across the wider zone is accommodated by displacement on small faults in the sandstone and ductile shear of shales shearing the rock in an inner damage zone. With continued shear displacement the deformation localizes to the fault-core with fault-rock development as shale smear and grain crushing or cataclasis. Fragments from the deformed protolith and the inner damage zone are incorporated into the fault-core.

As described, the outer damage zone may have small faults or fractures extending a short distance away from the fault-core. In porous, granular rock such as sandstones these small faults are often narrow deformation bands. In tighter cemented rocks with low porosity the deformation is more often fractures or joints that develop as open conduits to flow. Both deformation bands and fractures may occur in the same rock volume but under different conditions.

Deformation Bands

Deformation bands are narrow zones of localized deformation approximately 10 to 15 grains thick. The grains within the band are rotated, rearranged and or broken. The deformation localized in these bands may be compactional or dilational and with shear or without shear along the band length (Fossen et al., 2007). This deformation can be conceptualized as a band with some thickness, h, separating a medium of intact rock (Figure 8). In the case of a dilational band, the porosity and permeability within the band may be greater than that in the protolith outside the band with an increase in the thickness, h. These are not common, however. Compactional bands are more common and tend to form under higher mean effective stress with burial and have a porosity reduced relative to that of the protolith with a reduction in the thickness, h, and increase in the stress normal to the band, σ_{nn}. If the rocks are deformed with an adequate mean effective stress, the grains may break and fragment further reducing the permeability across the bands. Frequently we observe deformation bands with a component of shear displacement, γ, and either a dilation or compaction component with an increase or decrease of the band thickness, h, although compaction with shear is more common.

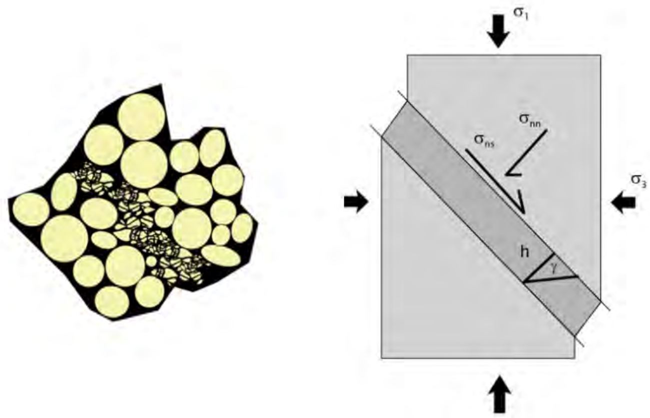

Figure 8. Left is a model of a deformation band in a porous sandstone with quartz grains in yellow. The deformation band is defined by the narrow zone of crushed grains. The image to the right is a model representation as a continuum representing the deformation across a deformation band.

It is common in outcrops to see sets of deformation bands along a similar trend forming an anastomosing architecture rather than a single long single trace (Hedgcoxe, 1987). A single width of deformation bifurcates along its length separating undeformed sandstone between two bands that come together or diverge again along the length. In three dimensions these lenses of undeformed sandstone separated by deformation bands likely form lenticular pods bounded on all sides by deformation bands. Following lengths of deformation bands in outcrops, however, show that they are discontinuous, like fault segments, and may terminate at stratigraphic interfaces or at some point along their length. An outcrop example of anastomosing deformation bands from the Entrada sandstone on the hike up to Delicate Arch is shown in Figure 9.

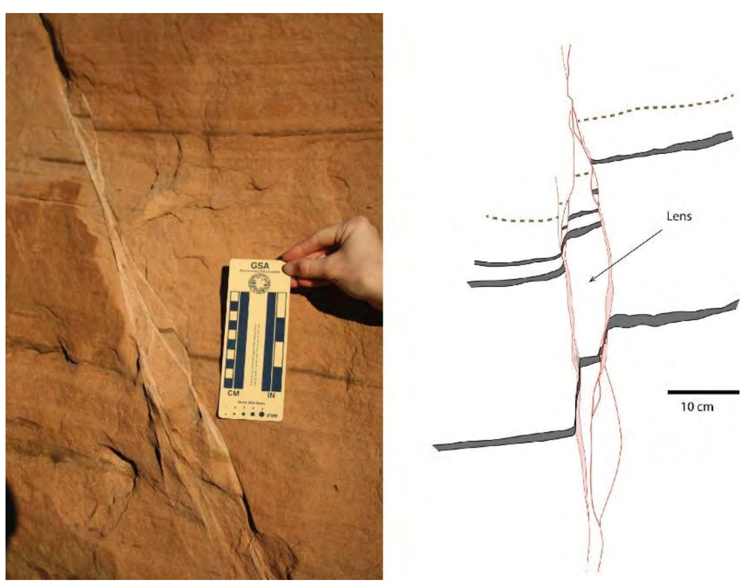

Figure 9. Outcrop photo and trace map of anastomosing deformation bands from the Entrada sandstone on the hike up to Delicate Arch. The dark layers are heavy minerals that show clearly the continuous shear across the deformation band.

Mode I Fractures

Fracture is a term applied in the oil and gas industry to refer to opening joints or breaks in the rocks with no shear and extension perpendicular to the fracture surface with an aperture that may be conductive to fluids. This is called a Mode I fracture. These fractures are common in tight rock with low porosity. For instance a fractured reservoir in oil and gas commonly refers to a granitic or tight carbonate that has no or low matrix porosity and the hydrocarbons are primarily stored and produced from fractures. These fractures, however, may be cemented with minerals precipitated from the fluids filling the apertures as in the example of calcite-filled fractures in a limestone from Oklahoma (Figure 10).

Figure 10. An outcrop example of a carbonate cemented limestone from Oklahoma.

Fractures also may occur in sandstone reservoirs, however. This seems perplexing as previously we stated that deformation bands form in porous sandstones as narrow zones with often fractured or crushed grains that impede flow and that fracture form in tight rocks as conduits to flow. There is no inconsistency as the style of deformation depends on the rock physics at the time of deformation. At shallow to moderate burial depths, sandstones maintain their porosity as the grains are compacted and slightly deform but preserve pore space. However, at greater depths of burial where subsurface temperatures exceed 100°C, the quartz at grain boundaries redistributes through pressure solution cementing the pores forming a low porosity and brittle sandstone. In this case, any differential stress applied to the rock will localize stresses at the tips of any microcracks in the rock like that in other rocks with a tight matrix. The cracks propagate across grains and link to form through-going open fractures (Figure 11). With shear across the fractures they may form small-offset faults.

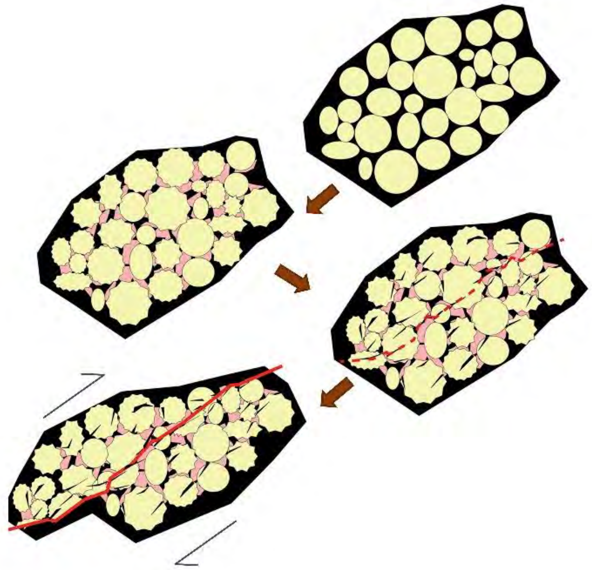

Figure 11. Conceptual model of a porous sandstone that is buried and cemented, subjected to a tectonic differential stress and deformated with the initiation and propagatoin of small fractures that form a through-going fracture that is subsequently sheared.

It should be evident from this discussion that in the same sandstone section we may observe deformation bands and fractures and that the deformation bands must have occurred prior to the fractures. The fractures occur after the sandstone has been buried with a significant loss of porosity from cementation increasing the rock strength and brittleness. We will observe both these styles of deformation at Stop 5C.

Fault Zone Architecture and Flow

With our model of the fault zone architecture, we can discuss the potential migration pathways of CO_2 or hydrocarbons across or up a fault. In this case, we assume no vertical migration pathways away from the fault through the pore space or fractures in an overlying caprock.

Consider a volume of CO_2 or hydrocarbon that migrates up dip through a reservoir such as the faulted Green River anticline (Figure 5) to the bounding Little Grand Wash and Salt Wash Faults but with a configuration in detail like that in Figure 6B. The fluid will first migrate to the outer damage zone. If a high frequency of deformation bands with lower permeability than the reservoir fill this zone, then the migration may slow but will unlikely stop because deformation bands rarely form a continuous linked cluster but have gaps along their lengths for fluid pathways. The low permeability deformation bands will retard the rate of flow.

Figure 12 is an example of a typical damage zone of deformation bands in the Entrada sandstone from Bartlett Wash along the Moab Fault north of Moab, Utah. The deformation bands extend approximately 60 meters from the fault-core but with an exponential decrease in the frequency or density. The deformation bands are not continuous but show discrete gaps between the clusters but also pathways for fluid migration around their tips.

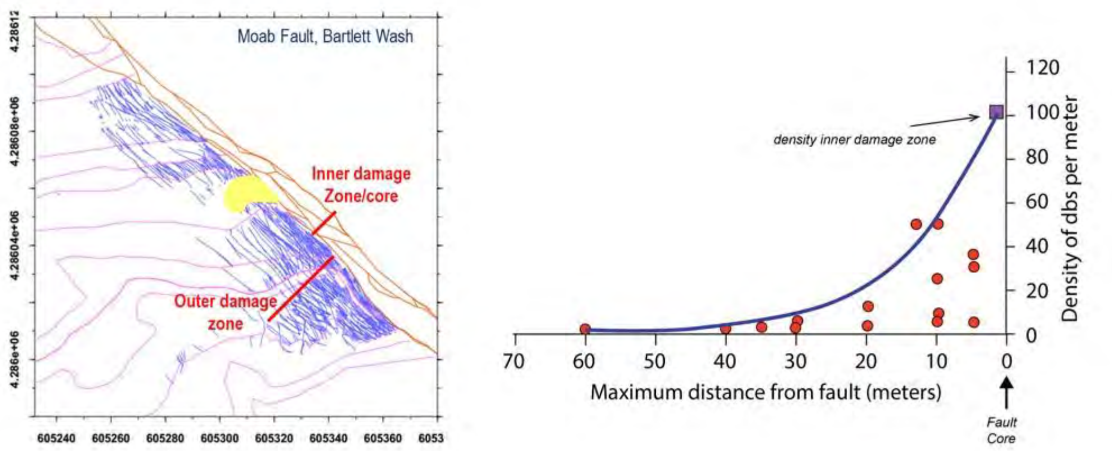

Figure 12. Left: Traces of deformation bands in the damage zone of the Moab Fault at Bartlett Wash Utah. Right: The exponential decrease in the frequency of the deformation bands away from the fault-core over 60 meters. The displacement across the fault is this location is approximately 300 meters.

If instead of deformation bands, the damage zone has a high frequency of linked open fractures, particularly that extend through the caprock, then the fluids may migrate up into shallower reservoirs or to the surface. A typical pattern and density of fracture traces in the damage zone is like that of deformation bands at Bartlett Wash (Figure 12).

If there is no vertical fluid loss through the damage zone, then the CO_2 or hydrocarbons will migrate to an inner damage zone. Faulted, brittle sandstone reservoirs surrounded by more ductile mudrocks typically develop an inner damage zone where the reservoir is sheared into the fault-core along small offset faults. Fluids migrate up dip into the sheared sandstones within the fault zone. The sandstone within the inner damage zone is attenuated and extends a short distance up the fault, which is a principal limiting factor in the continued up-fault migration in the more porous sandstone. Gouge or fault-rock developed along the faults from the deformed protolith may have low permeability and further resist the upward migration.

Whether the fault has a damage zone or not, the principal control on the cross fault flow and limits on up-fault flow is the fault-rocks in the fault-core. The fault-rock is a gouge of cataclastic rock from the more brittle section of protolith or a smearing of more ductile lithofacies derived from the protolith. The greater the cataclasis or grain breakage and higher the clay content the lower the permeability and creation of a cross-fault seal. There are many publications related to the calculation of clay content along the fault to predict the cross-fault seal risk including shale gouge ratio (SGR; Yielding et al, 1997) and clay smear (Vrojlik et al., 2016).

Areas along the fault with low clay content are more likely to provide pathways for fluid migration across the fault. If a non-reservoir is juxtaposed against the reservoir across the fault this can act as a juxtaposition seal.

If the fluids get into the fault-core they can migrate up the fault but are limited again by the petrophysical properties of the fault-rock. The fault-core is narrow, and the associated fault-rock a heterolithic discontinuous mixture. Fluids that get into the fault-core may migrate a short height above the trap crest but the height is limited by lower permeability fault-rock within the fault-core.

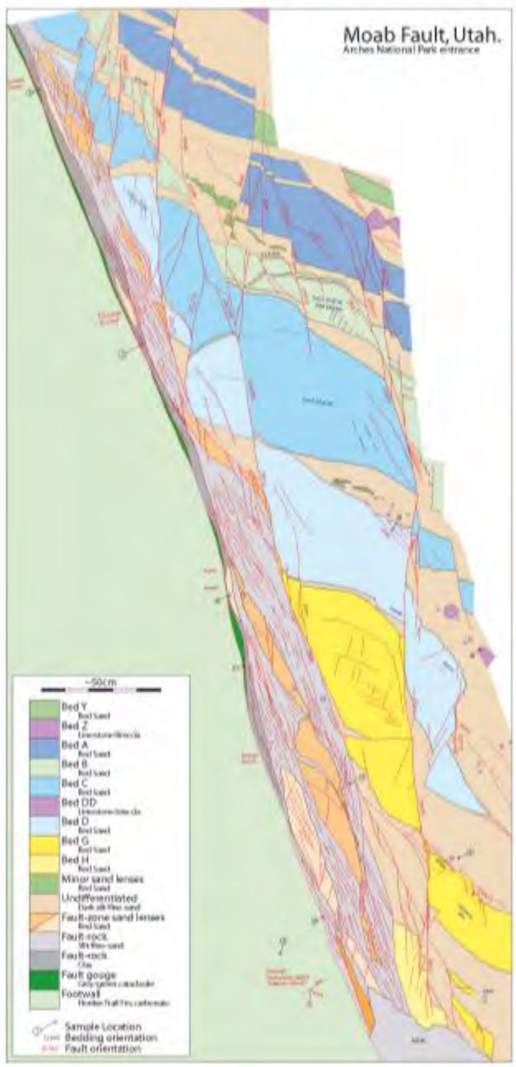

Figure 13. Moab Fault deformation near entrance to Arches National Park showing inner damage zone and narrow clay rich fault-core against a fault bounding surface of Honaker Trail Formation shown in green. The scale bar is 50 cm.

Slip surfaces within the fault-core can provide fluid pathways but these are not typically open in the subsurface because of high mean effective stress. Active slip on these slip surfaces from seismic activity can provide temporary pathways and episodic fluid loss (Barton et al., 1995).

Fault Zone Example: Moab Fault

An excellent example of an inner damage zone and core is from the Moab Fault near the entrance to Arches National Park in the small wash between the main route 191 and the park road (Figure 13). At this location the fault has a displacement of up to 1 km. The triangular region to the left in the figure is the fault surface against the Honaker Trail section in the fault footwall that is rotated and attenuated but not mapped in detail. Further to the right or south of the figure the stratigraphy is nearly flat and then rotates into an inner damage zone within the fault shear zone as mapped. The rotation of the intact layered stratigraphy in the inner damage zone is shown by the yellow, blue and purple sandstone layers separated by the tan siltstones. The stratigraphy of these sandstones and siltstone remains intact but is offset across small faults that shear and attenuate the layers towards the fault-core. Kinematically this layered and sheared section is displaced downwards along the fault in the figure. With displacement some of the layers are completely offset from each but others are still self-juxtaposed. If fluids migrate from the protolith to the left into the fault they could migrate up into this inner damage zone but the upward migration would be limited by cross-fault flow resistance and juxtapositions of the small throw faults and the limits of the separate sandstone layers up the fault.

Between this inner damage zone and the fault surface against the Honaker Trail Formation is a thin 10 to 20 cm wide fault-core of a clay rich smear or gouge with lenses of attenuated and broken sandstone. This fault-rock of low permeability gouge is the principal resistance to cross-fault and up-fault flow.

This discussion of the fault zone architecture and fluid migration provides insight as to the limits of fluid migration in the fault-core and that a more reliable pathway for vertical migration of fluids up the faults is in open fractures in the outer damage zone. Open Mode I fractures, however, are not limited to fault damage zones and may nucleate and propagate across brittle rocks such as cemented sandstones in response to a differential stress related to local folding, for example. These Mode I fractures may be closed in the subsurface and require a seismic event across the fault zone or pore pressure for an episodic opening and fluid loss vertically.

We can consider this model of the fault zone, local deformation and fluid migration to discuss the fluid flux as observed along the faults and trap in the Green River anticline.

Fluid Migration: Green River Anticline

We previously discussed a CO_2 source from deeper horizons in the Green River Anticline that migrated upwards into shallower Jurassic Navajo and Entrada sandstone reservoirs and to the surface. The migration pathways are less certain, however, as the CO_2 may migrate upwards through pore throats and fractures in the layered stratigraphy, Mode I fractures in the outer damage zone or up the fault-core. The expectation from structural trap geometry of the Green River Anticline, however, is that the buoyant fluids would migrate vertically, up-dip and fill against the faults if they seal (Figure 5).

If the faults do not seal to cross-fault flow the CO_2 would leak across the faults to the hanging wall of the Salt Wash Faults and presumably escape to the surface with no preserved volume. If the faults bounding the north and south plunging noses of the anticline are sealing along their full length the CO_2 would fill the entire separate Little Grand Wash and Salt Wash trap closures to their respective lowest spill points. Neither of these scenarios of leak or seal seem to accurately represent the observed CO_2 in the trap at the Green River Anticline.

The strongest evidence for CO_2 across the anticline is from active geysers, springs and travertine deposits at the surface and from well data in the subsurface. The geysers described are associated with abandoned well bores. Wells drilled near the crest of the structure have evidence of CO_2 in the Jurassic reservoirs, the Entrada and Navajo sandstones. The springs and travertine deposits described are aligned along the fault traces bounding both the crest of the Little Grand Wash and Salt Wash closures as shown by the stars on the geological and structure map (Figure 3 and Figure 5 and Plates 1 and 2). The surface locations of CO_2 flux are limited to the structural crest. If the entire trap were filled to spill we might expect a broader range in locations of CO_2 at the surface. In fact, we can hypothesize that the present day maximum fill height of CO_2 is from the structural crest to the structural closures as defined by the springs or deposits furthest downdip. This column height is approximately 50 to 75 meters. It is possible that in the past the faults supported a greater height of CO_2 but that the trap has been breached either by migration through the caprock pore throats or fractures or along the fault further down dip than the present day limits. The present estimate of the height of CO_2 column may be controlled by cross-fault leak in the fault-rock in the fault-core, juxtaposition of reservoirs across the fault, or vertical leakage through the overlying low permeability lithofacies or conductive fractures.

The CO_2 at the surface has been described in the fault footwall, which is expected if the volume does not extend much downdip. If juxtaposition seal is the control on the column of CO_2 a cross-fault sealing lithology is expected to the height of column. Low permeability fault-rocks, however, may also control the column height even if the reservoirs are juxtaposed across the fault. A systematic analysis of these fault controls is possible but requires a good 3D model of the faults and an accurate stratigraphic model of juxtaposition against the fault.

The faults have complex tip interactions from their mapped traces, outer damage zones comprised of deformation bands and open fractures and complex inner damage zones of rotated and sheared beds adjacent to the fault. Detailed mapping by Vrolijk et al, (2005) discussed in the GSA field guide along the Little Big Wash Fault showed that the fault complexity increased with an increase in the layering or Vertical Mechanical Heterogeneity consistent with the fault zone model discussed.

Detailed outcrop studies from the Little Grand Wash Fault show evidence that CO_2 migration is limited to the fault zone in the footwall at the structural crest based on observed carbonate-filled fracture distributions, springs and travertine deposits (Urquhart, 2011). There is no clear evidence of more widespread cemented fractures or travertine or springs away from the fault. Although there are fewer studies describing the CO_2 flux along the Salt Wash Graben faults, the observations suggest here a similar concentration of CO_2 in the footwall although it is less evident that the CO_2 is constrained to the fault zone and more widespread distribution of CO_2 is possible.

Many of the fractures in the outer damage zone on the footwall of the Little Grand Wash Fault are cemented. Geochemical analysis of the cements and fluids from the fractures at the Little Grand Wash Fault have shown that the likely fluid migration pathway favors these fractures in the damage zone with no evidence of migration up the fault-core. This is also consistent with our previous discussion on the fault zone mechanisms. The deformation bands in the damage zone would have occurred early and the fractures later. This area was rapidly uplifted on the Colorado Plateau 5 to 10 Million years ago, for instance. The burial and subsequent uplift are ideal conditions that favor stress reduction and fracture propagation. Vertical migration and loss may occur together with active charge filling the reservoirs; a balance of charge and loss.

Local stress perturbations across the structure from changes in tectonic stress or local deformation from deeper salt migration can also deform the rocks away from the fault. The deformation styles will depend on the rock physics at the time of deformation. Sets of deformation bands may develop across the structure where the sandstones are porous prior to deep burial. Differential stress applied to the rocks that are more brittle and strong from greater cementation of the pores will develop Mode I fractures. The timing of the fracture development may vary as a function of the tectonic history from burial to uplift.

We will have the opportunity to observe the fault zone architecture and deformation styles in the rocks at Stop 5C and Stop 7 and 9 along the northern bounding faults of the Salt Wash and Ten Mile Grabens. At Stop 5C, beds are rotated into the fault-core and both deformation bands and fractures are evident. A key question is whether this observed deformation is from the fault activity or local stress perturbations not associated with faulting, and the timing of the deformation. The timing is important relative to the separate set and styles of deformation but also the fluid migration.

This location is downdip of the structural crest and our cursory observations are that fractures show no evidence of mineralization. There is no known spring or travertine deposit described along this lower contour interval of the trap (Figure 5 and Plate 2), but it is possible that fluids migrated through these rocks at an earlier time and the trap was breached.

Stop 9 is at the crest of the structure where there is strong evidence of present day flux from springs and travertine deposits. A key observation is determining evidence of cementation in fractures and if so where is this relative to the fault, for instance in the damage zone or elsewhere across the rock volume? The cementation process is discussed elsewhere in the field guide.

Migration Model

The cross-section in Figure 14 is along the axis to the Green River Anticline with the general migration pathways discussed of deeper charge of CO_2 migrating up through the overlying section and up dip to the fault where open fractures may provide a lower resistance pathway to shallower reservoirs capped by intra reservoir seals. This up-dip migration is consistent with the cemented fractures along the damage zone of the Little Grand Wash Fault. The CO_2 may fill the Navajo and Entrada sandstone reservoirs increasing the column of CO_2 and the buoyancy pressure against the caprock. This buoyancy pressure may eventually exceed the capillary threshold pressure of the seal or migrate through Mode I fractures across the structure migrating to shallower stratigraphic layers and to the surface. We should look for evidence of vertical migration away from the faults as evidence of this process although more likely is the migration to the fault at the structural crest. At this location the buoyancy pressure will be greatest with the greatest chance of breaching the seal and migrating to the surface. The question is by what mechanism is the fluid leaking, through the pore spaces in the caprocks or along fractures or faults?

A cross-fault seal of juxtaposition against a sealing lithology or low permeability fault-rocks may provide adequate resistance to build a column of CO_2 in the reservoirs prior to upward migration at the structural crest. We would expect that if the Mancos Shale were buried at this location it would act as a regional seal and prevent the migration of the CO_2 to the surface.

This model is conceptual and excludes a detailed stratigraphy. During the field trip we have opportunities to view the stratigraphic heterogeneity, which one should consider in controlling the deformation styles dependent on the rock properties, the reservoir or sealing properties for fluids and their impact on fault zone architecture.

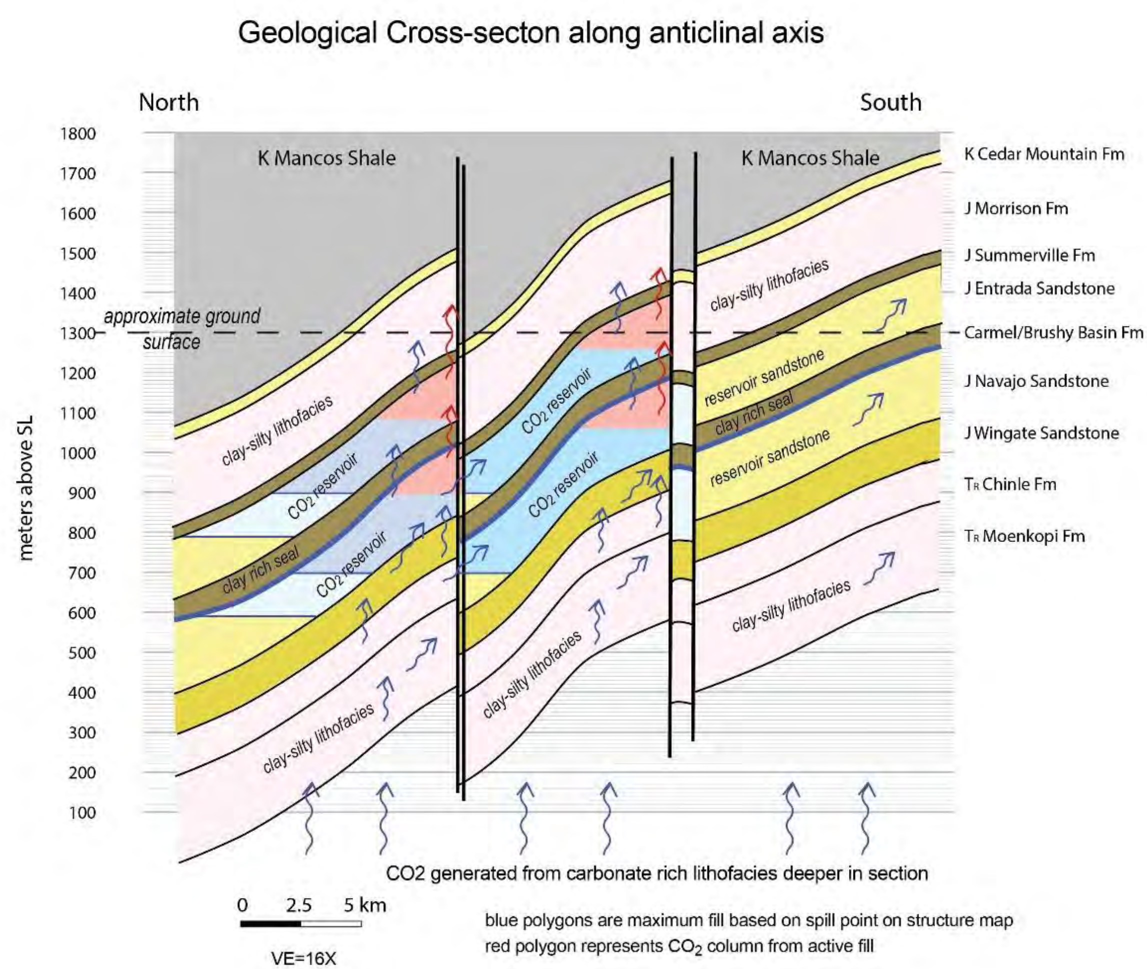

Figure 14. Cross-section across the axial trace of the Green River anticline (Figure 5) with approximate formation thicknesses and inferred fill to spill limits from closed contours on structure map. The arrows show deeper charge of migrating CO_2 up into shallow reservoirs with potential migration pathways.

Faulted Outcrop Observations (Stops 5C, 7 and 9)

Topics

- Fault Zone Architecture
- Deformation Styles
- Evidence of Fluid Migration

Description

During the field trip at Stops 5C, 7 and 9 (Figure 15) we will have the opportunity to observe the detailed architecture of the faults along the Ten Mile Graben and Salt Wash Grabens that bound the upper crest of the plunging Green River anticline. The faults all have normal offset and are the northern bounding faults to the narrow grabens and dip to the south.

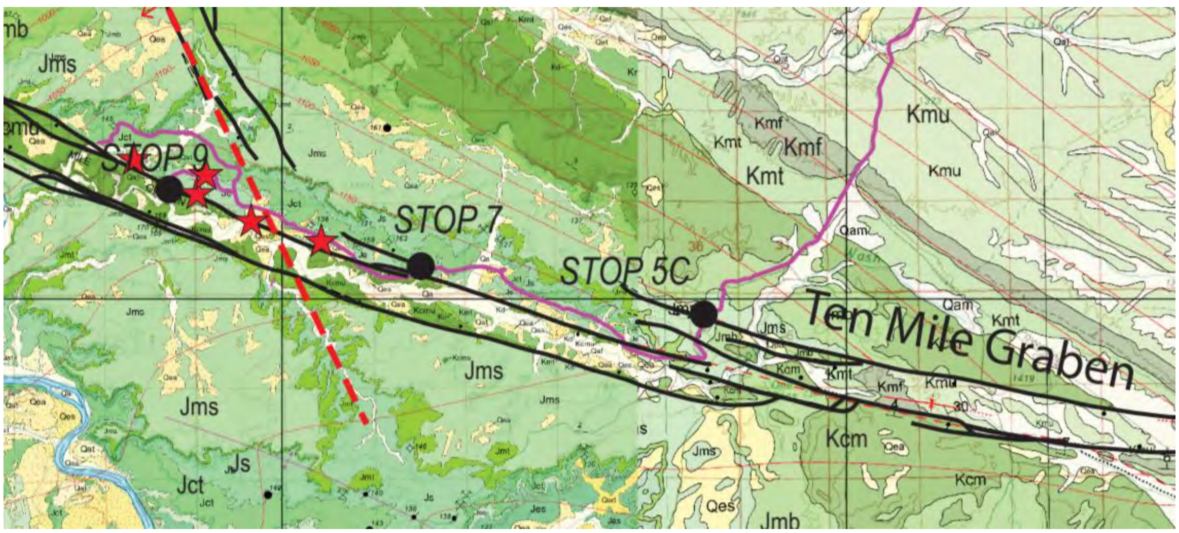

Figure 15. Geological map with route track in purple and locations of key stops for studying the fault zones.

At these locations consider the fault model presented in Figure 6B and look for evidence of the outer damage zone, inner damage zone and fault-core.

What is the deformation style in the outer damage zone? Do you see deformation bands, Mode I fractures or both? If there are fractures, are they filled with cement and what is their location relative to the structure? What is the timing of the fractures relative to the deformation bands?

Is their evidence of Mode I fractures or deformation bands that are not associated with the damage zone? What is their spacing? Is it regular or decreases in density away from the fault-core?

Is there any indication of an inner damage zone? Is this in the footwall or hanging wall or both and if observed does it seem to play a role in the fluid migration?

Can you see a fault-core of fault-rocks? Is there evidence of fluids migrating through the fault-core?

Is their evidence of fluids migrating to the surface either hydrocarbons or CO_2 and where are these fluids relative to the larger trap geometry and to the fault? Are the fluids observed in the footwall or hanging wall of the fault or both? Are the fluids in the fault zone or across the structure away from the fault?

Stop 5C (Figure 15 and Plate 1)

Ten Mile Graben Fault

(Lat. 38.842709°; Lon. -109.991705 °; Elev. ~4467 ft)

At this location we will have an opportunity to view a normal fault and the detailed fault zone architecture and outer and inner damage zone and other small scale deformation including deformation bands and Mode I fractures. The fault-core is more difficult to see because of the erosion and fill.

The fault is the northern bounding fault of the Ten Mile Graben approximately 1.5 km from its western tip (Plate 1 and Figure 15). The fault is oriented ESE-WNW and the road cuts across the strike of the fault. Figure 16 is an aerial drone view showing a perspective view of the fault and the stratigraphic contacts looking both east and west. Some of the more competent sandstones such as the Salt Wash Member of the Morrison Formation are well preserved but much of the stratigraphy along the fault is eroded limiting detailed observations of structural styles and deformation. Note that in the view to the west, two fault segments form a small overlap and hard link to the west.

At this location consider the model of fault-zone architecture (Figure 6) and try and identify outer damage zone, inner damage zone and fault-core. What are the structural styles? What do you think about timing of the structures? Is their evidence of cross-cutting relationships? Is there evidence of mineralization in any fractures or pores? Is the deformation different for the different lithofacies? Is there evidence of staining in the rock?

Figure 16. Drone views east and west along the northern bounding fault of the Ten Mile Graben taken from the road. Drone photograph by Rex Cole. Mode I fractures are clearly visible across the Salt Wash sandstone.

There are a few locations along the fault trace where deformation in the outer damage zone is exposed. The left image in Figure 17 is a perspective view from a drone photograph near the road looking south that shows the trace of the fault in red. A second minor fault is interpreted further south. Brann Johnson is at the intersection of the main fault trace and the pipeline for scale.

Figure 17. Left: Perspective view looking south where the red trace is the fault crossed by the pipeline. Brann Johnson is at the fault contact crossed by the pipeline for scale. Right: Drone image looking down at a zone of deformation bands in the Salt Wash sandstone at the location of Brann Johnson in the left figure. The pipeline is in the upper left. Drone photos by Rex Cole.

The blocky sandstone in the upper right (Figure 17 – left) is the Salt Wash Member of the Morrison Formation in the footwall or upthrown side of the fault juxtaposed against the Brushy Basin Member of the Morrison Formation in the hanging wall. The heterolithic siltstone, sandstones and mudrocks in the hanging wall are rotated (dipping southward) up against the fault-core as representative of deformation in the inner damage zone.

Near the location of Brann Johnson in the figure are sets of deformation bands (Figure 17 - right). The location of these deformation bands is consistent with the outer damage zone and are closely-spaced and oriented sub-parallel to the strike of the main fault. If these are related to the fault evolution they would have formed when the rock was porous without significant cementation between the grains. Deformation bands, however, may also form across the structure not associated with fault evolution from local stress perturbations including folding. Is there evidence of deformation bands in this area away from the fault? Does the spacing or density of deformation bands in this location decrease away from the fault-core? Are these sets of deformation bands consistent with our description of an outer damage zone?

A drone image looking down upon a channel sandstone deposit of the Salt Wash Member of the Morrison Formation further along the fault to the west (Figure 18; see Figure 16 top for location) shows a set of Mode I or open fractures with a strike also sub-parallel to the strike of the main fault. These fractures are close to the fault trace and may be in the outer damage zone of the footwall. However, they extend much further than the width of a typical outer damage zone and are evenly spaced suggesting a more regional joint set. There are other similar fracture sets across the Salt Wash sandstone across the structure suggesting that they may have formed under different stress conditions than the faulting such as folding. Migration of the Paradox salt has been interpreted to deform the overlying section nucleating regional fractures sets (Lorenz and Cooper, 2009).

The timing of the Mode I fractures and the deformation bands is important. Deformation bands are a typical deformation mechanism in porous, granular media such as sandstone. Sandstones can maintain their porosity to depths as great as 3 km. At deeper depths and greater temperatures, however, the pores are cemented and the rock becomes stronger and brittle. These rocks subjected to differential stresses will deform by the development of Mode I fractures. The fractures are later than the deformation bands but the exact timing is difficult to determine. Some of the fractures across the Salt Wash sandstones in these locations may have occurred after the uplift of the Colorado Plateau and be more recent.

Mode I fractures are also evident in cross-section in the Salt Wash Sandstone exposed in the upper right in Figure 17. We can observe the orientation and vertical extent of these fractures in cross-sectional view (Figure 19).

Figure 18. Drone photo of fractures in the fault footwall of Salt Wash sandstone. The location of this outcrop can be seen along the fault footwall in the central part of the drone photograph in the upper image in Figure 16. Drone photograph by Rex Cole.

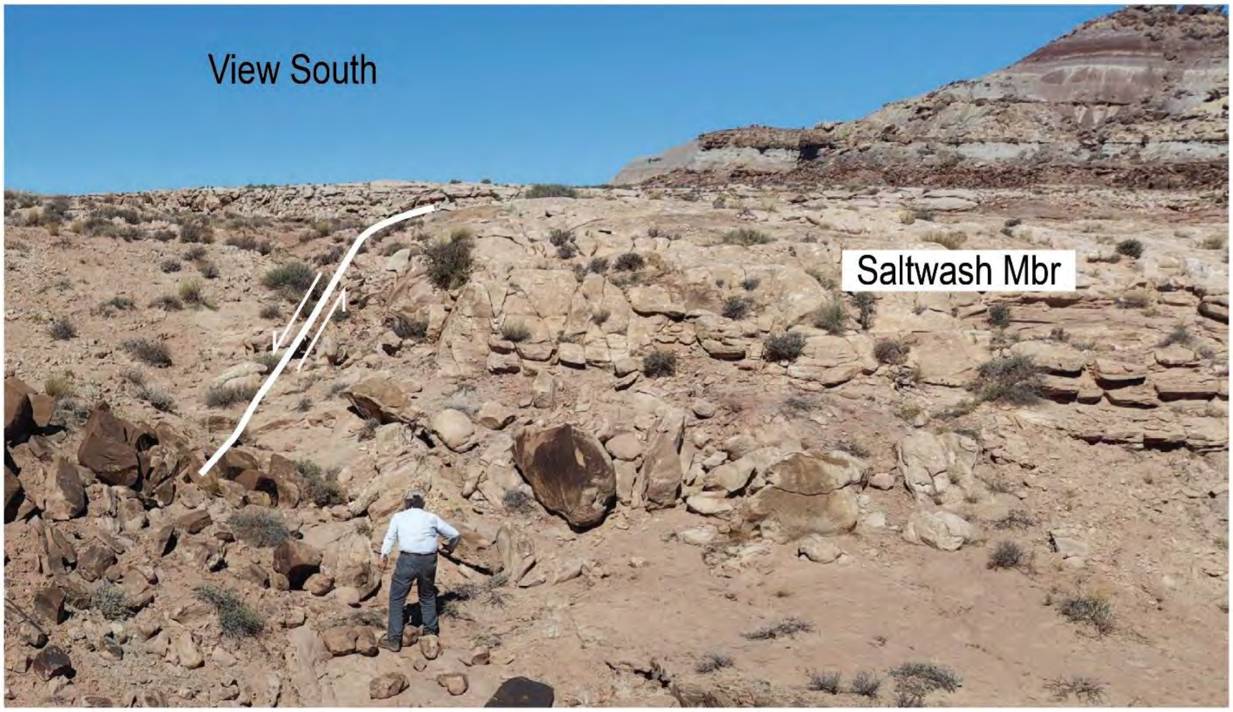

Figure 19. Cross section showing the extent of fractures and their orientation across a channel sandstone in the Salt Wash Member of the Morrison Formation. The outcrop location is along the fault west of the pipeline in the upper right of the drone photograph in the left image in Figure 17. Drone photograph by Rex Cole and Brann Johnson for scale.

This field location is within the anticlinal closure of the faulted Green River Anticline (Plate 2) but far down dip and beyond the surface evidence of CO_2 flux from springs or travertine deposits. Our cursory observation at this stop is that the fractures are uncemented and that there are no springs or travertine deposits. This might suggest that the CO_2 did not extend to this depth along the trap but we suggest looking for evidence of any fracture fill to challenge this hypothesis. We will discuss the trap scenarios at Stops 7 and 9 closer to the crest of the structure where there is evidence of springs and travertine deposits.

As we leave Stop 5C we continue to drive a short distance south perpendicular to the fault strike across the northern bounding fault to the Ten Mile Graben, into the graben and the across the southern bounding fault into a relay separating the Ten Mile Graben from the Salt Wash Graben (Figure 15; Plates 1 and 2).

At the northern bounding fault to the Salt Wash Graben the road turns to the west and takes us along the strike of the northern bounding fault to the Salt Wash Graben dropping from footwall to hanging wall at several places. As we drive consider the fault zone architecture and stratigraphic controls.

Stops 7 and 9 (Figure 3 and Plate 1)

Salt Wash Graben Fault:

Stop 7 (Lat. 38.8506º; Lon. -110.0496º; Elev. ~ 4,280 ft)

Stop 9 (Lat. 38.8647º; Lon. -110.1076º; Elev. ~ 4,110 ft)

Field Stops 7 and 9 place us again close to the normal fault but in this case the northern bounding fault dipping south to the Salt Wash Graben. A perspective drone view looking west shows the stratigraphic juxtapositions across the fault and overall structural style (Figure 20).

Stop 7 is the lower limit beyond the recorded surface evidence of CO_2 flux but look for any evidence of filled fractures, spring or travertine. Stop 9 is well within the area of springs, geysers and travertine. Does the damage zone show evidence of fluid migration in the outer damage zone or is there other evidence of fluid migration pathways?

At each Field Stop keep in mind the fault styles and particularly the detailed deformation. Note also that many of the sandstones are red from the oxidation of the iron rich hematite coatings on sand grains but that in places the sandstone is bleached. Bleached halos are also evident around many of the cemented fractures.

The bleaching has been attributed to a reducing fluid such as hydrocarbons that dissolve the iron oxide removing it from the grain coatings. Bleached sandstone around Moab has been attributed to breached hydrocarbon traps (Chan et al., 2000).

In this field area, the CO_2 may acidify the groundwater forming carbonic acid that under appropriate conditions react with the iron bleaching the rock. If the fluid pathways are open fractures, the bleaching halos are evidence of a zone of migration and fluid-rock interaction. Detailed analysis of diagenesis along fractures including CO_2 has been well documented along the Moab Fault (Eichhubl et al., 2009).

Figure 20. Drone perspective view to the west along the Salt Wash Graben fault from Field Stop 7, Drone photograph from Rex Cole

References

Barton, C.A., Zoback, M.D., Moos, D. and Sass, J.H., 1995, June. In-situ stress and fracture permeability in the Long Valley Caldera. In ARMA US Rock Mechanics/Geomechanics Symposium (pp. ARMA-95). ARMA.

Caine, J.S., Evans, J.P. and Forster, C.B., 1996. Fault zone architecture and permeability structure. Geology, 24(11), pp.1025-1028.

Chan, M.A., Parry, W.T. and Bowman, J.R., 2000. Diagenetic hematite and manganese oxides and fault-related fluid flow in Jurassic sandstones, southeastern Utah. AAPG bulletin, 84(9), pp.1281-1310.

Davies, R.K., Crawford, M., Dula Jr, W.F., Cole, M.J. and Dorn, G.A., 1997. Outcrop interpretation of seismic-scale normal faults in southern Oregon: description of structural styles and evaluation of subsurface interpretation methods. The Leading Edge, 16(8), pp.1135-1142.

Doelling, H.H., 2002. Geologic map of the Moab and eastern part of the San Rafael Desert 30'x 60'quadrangles, Grand and Emery Counties, Utah, and Mesa County, Colorado. Utah Geological Survey.

Doelling, H.H., Kuehne, P.A., Willis, G.C. and Ehler, J.B., 2015. Geologic map of the san Rafael Desert 30'x 60' quadrangle, Emery and Grand Counties, Utah. Utah Geological Survey.

Eichhubl, P., Davatz, N.C. and Becker, S.P., 2009. Structural and diagenetic control of fluid migration and cementation along the Moab fault, Utah. AAPG bulletin, 93(5), pp.653-681.

Fossen, H., Schultz, R.A., Shipton, Z.K. and Mair, K., 2007. Deformation bands in sandstone: a review. Journal of the Geological Society, 164(4), pp.755-769.

Hedgcoxe, H.R., 1987. Development of secondary faults between en echelon, oblique-slip faults: examples from basement controlled, small-fault systems in the Llano Uplift of central Texas (Doctoral dissertation, Texas A&M University).

Jung, N.H., Han, W.S., Han, K. and Park, E., 2015. Regional-scale advective, diffusive, and eruptive dynamics of CO2 and brine leakage through faults and wellbores. Journal of Geophysical Research: Solid Earth, 120(5), pp.3003-3025.

Kampman, N., Bickle, M.J., Maskell, A., Chapman, H.J., Evans, J.P., Purser, G., Zhou, Z., Schaller, M.F., Gattacceca, J.C., Bertier, P. and Chen, F., 2014. Drilling and sampling a natural CO2 reservoir: Implications for fluid flow and CO2-fluid–rock reactions during CO2 migration through the overburden. Chemical Geology, 369, pp.51-82.

Lorenz, J.C. and Cooper, S.P., 2009. Extension-fracture patterns in sandstones above mobile salt: the Salt Valley Anticline, Arches National Park, Utah.

Shipton, Z.K., Evans, J.P., Kirschner, D., Kolesar, P.T., Williams, A.P. and Heath, J., 2004. Analysis of CO2 leakage through 'low-permeability' faults from natural reservoirs in the Colorado Plateau, east-central Utah.

Shu, Y., 2018. Natural analogues for geological carbon storage. PhD thesis University of Edinburgh

Urquhart, A.S.M., 2011. Structural controls on CO_2 leakage and diagenesis in a natural long-term carbon sequestration analogue: Little Grand Wash fault, Utah.

Vrolijk, P., Myers, R., Sweet, M.L., Shipton, Z.K., Dockrill, B., Evans, J.P., Heath, J. and Williams, A.P., 2005. Anatomy of reservoir-scale normal faults in central Utah:: Stratigraphic controls and implications for fault zone evolution and fluid flow.

Vrolijk, P.J., Urai, J.L. and Kettermann, M., 2016. Clay smear: Review of mechanisms and applications. Journal of Structural Geology, 86, pp.95-152.

Williams, A.P., 2004. Structural analysis of CO2 leakage through the Salt Wash and Little Grand Wash faults from natural reservoirs in the Colorado Plateau, southeastern Utah.

Yielding, G., Freeman, B. and Needham, D.T., 1997. Quantitative fault seal prediction. AAPG bulletin, 81(6), pp.897-917.

Geological Map
Green River Anticline

Modified from Doelling et al., 2015 and Doelling, 2002

PLATE 1

Structure Map on top Navajo Sandstone
Green River Anticline

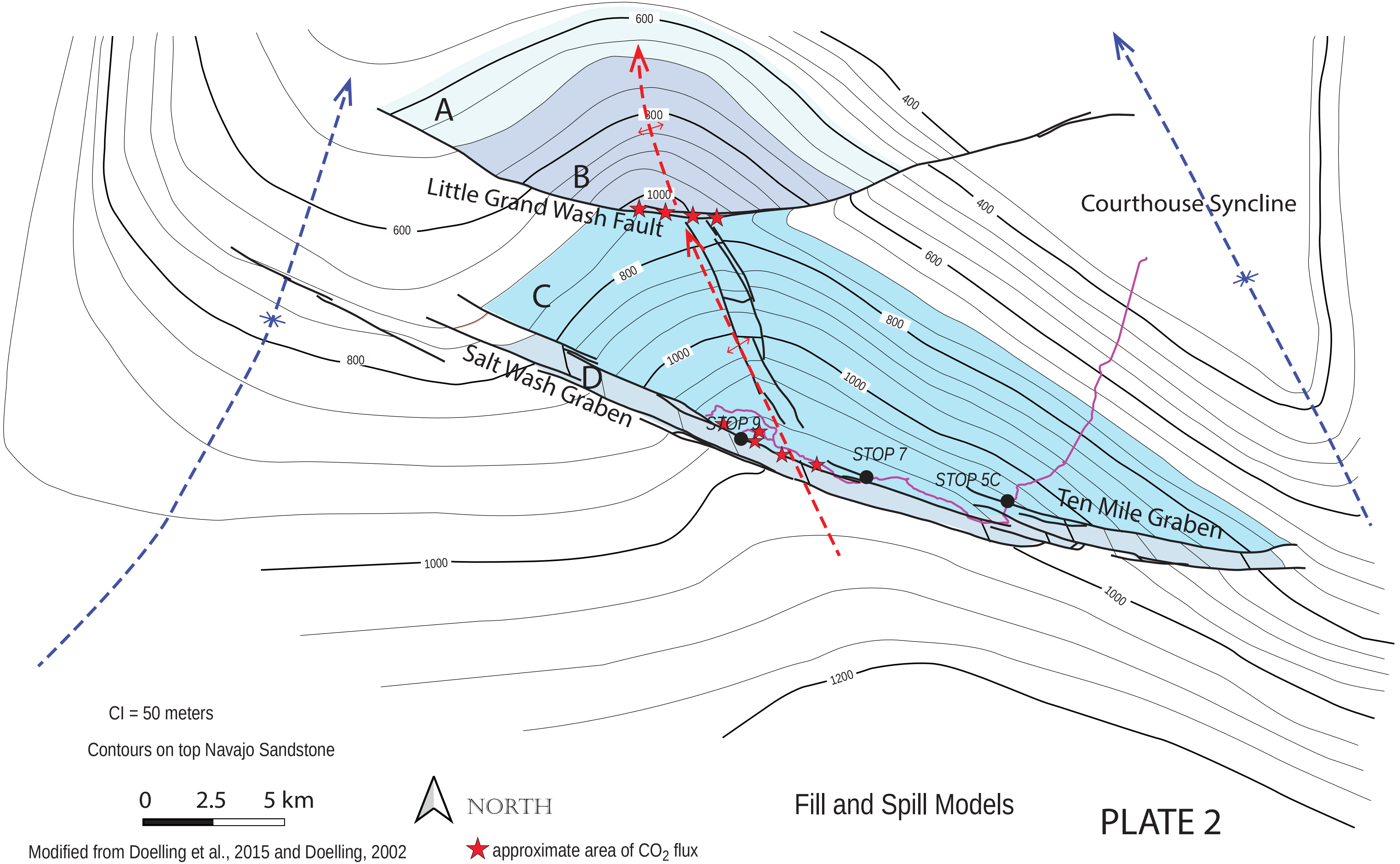

Modified from Doelling et al., 2015 and Doelling, 2002

Fill and Spill Models

PLATE 2